WAPD-TM-1425

DOE Research and Development Report

Evaluation of the Mechanical Properties of an Irradiated, Type 347 Stainless Steel, In-Pile Tube with a Peak Fluence of 4×10^{22} n/cm^2 (>1 Mev)

J. J. Krupowicz

Bettis Atomic Power Laboratory
West Mifflin, Pennsylvania 15122

August 1979

Prepared for the
U.S. Department of Energy
By Westinghouse Electric Corporation
Under Contract No. DE-AC11-76PN00014

DISCLAIMER

EVALUATION OF THE MECHANICAL PROPERTIES OF AN IRRADIATED TYPE 347 STAINLESS STEEL IN-PILE TUBE WITH A PEAK FLUENCE OF 4×10^{22} n/cm^2 (>1 Mev)

J. J. Krupowicz

August 1979

Contract DE-AC11-76-PN00014

Printed in the United States of America
Available from the
National Technical Information Service
U. S. Department of Commerce
5285 Port Royal Road
Springfield, Virginia 22151

NOTE

This document is an interim memorandum prepared primarily for internal reference and does not represent a final expression of the opinion of Westinghouse. When this memorandum is distributed externally, it is with the express understanding that Westinghouse makes no representation as to completeness, accuracy, or usability of information contained therein.

BETTIS ATOMIC POWER LABORATORY WEST MIFFLIN, PENNSYLVANIA
Operated for the U.S. Department of Energy
Westinghouse Electric Corporation

0128/79-650

CONTENTS

TABLES

FIGURES

Abstract

This report presents the results of post-irradiation mechanical testing of Type 347 stainless steel specimens machined from an Engineering Test Reactor in-pile pressure tube. Tests included tensile and fracture toughness at room temperature, 600°F, 800°F, and 1000°F, room temperature fatigue, and delayed failure stress rupture with stresses approaching the yield stress. Immersion density measurements were also made. Specimen fluences varied up to 4×10^{22} n/cm^2 (>1 Mev). Although irradiation increased the strength, the material remained ductile and showed no evidence of notch or strain rate sensitivity, or embrittlement. Static and dynamic fracture toughness values were well above the minimum failure criterion requirements. At higher fluences all of the mechanical properties appear constant, indicating saturation of the irradiation damage. Extended in-pile service of such in-pile pressure tubes to 4×10^{22} n/cm^2 (>1 Mev) was justified.

EVALUATION OF THE MECHANICAL PROPERTIES OF AN IRRADIATED TYPE 347 STAINLESS STEEL IN-PILE TUBE WITH A PEAK FLUENCE OF 4 x 10^{22} n/cm^2 (>1 Mev)

I. Introduction

In-pile pressure tubes (IPT's) are used in test reactors for the purpose of containing specimens of fuel or other test materials during irradiation. Because of the proximity of the IPT's to the core, they are irradiated to extremely high fluences. The Engineering Test Reactor (ETR), now shutdown, contained Type 347 stainless steel IPT's, while the currently operating Advanced Test Reactor (ATR) uses Type 348 material. Numerous investigations have characterized the effects of neutron irradiation on many engineering materials, but data on Type 347 stainless steel irradiated to very high fluences are limited. Although a worst case (catastrophic), in-service failure due to internal pressure of an IPT would not result in degradation of public health and safety (a hazard analysis has been performed), such an event is clearly undesireable. Any experimental specimens in the tube would probably be ruined, making such an occurrence even more costly and undesireable. The premature removal and replacement of the tubes is time consuming and extremely expensive. Thus, maximum lifetime for each tube is desireable. Assessment of the integrity of the IPT's for continued service has required that, periodically, irradiated pressure tubes be subjected to various destructive tests at successively higher fluences. Results of these tests have been used to justify incremental increases in the in-pile tube fluence limits.

In the Advanced Test Reactor (ATR), the fluence limit for the Type 348 stainless steel IPT was 3 x 10^{22} n/cm^2 (>1 Mev). In the Engineering Test Reactor (ETR), IPT's were permitted exposure to a maximum fluence of approximately 4 x 10^{22} n/cm^2 (>1 Mev) and were available for destructive testing. Differences in the operating conditions and materials of the ETR and ATR IPTs are not considered significant in evaluating the effects of irradiation. Thus, data from an ETR tube are judged to be directly applicable to ATR and can be used, if favorable, to extend the IPT fluence limits in ATR. To this end, a program was initiated to destructively test one Type 347 stainless steel IPT from ETR irradiated to a maximum fluence of approximately 4 x 10^{22} n/cm^2 (>1 Mev), and to use the results, if favorable, to justify an extension of the current ATR IPT fluence limits. This report presents the mechanical test results of the Type 347 stainless steel IPT performed from 1975-1976.

II. Background

A. ETR and ATR IPT Details

A schematic illustration of the ETR Type 347 stainless steel IPT is shown in Figure 1. The hot segment lay within the core of the reactor with the cold segment adjacent to the core. The cross sectional dimensions of these segments are 2.530 in. OD by 2.125 in. ID. The ATR IPT's are of the same size as those of ETR. The inside of the pressure tube is pressurized to prevent boiling with purified water containing < 0.1 ppm chloride and < 0.14 ppm oxygen so as to minimize corrosion problems. Pressures, as well as operating temperatures for the ETR and ATR high fluence regions, are as follows:

	ETR	ATR
Pressure, psi		
Design	2500	2500
Operating	2250	2200
Temperature, °F		
ID	Not Available	625
OD	Not Available	808
Mean	703	725

A thermally insulating gas jacket surrounds the IPT. This jacket provides water containment in the event of a tube failure. The annular space between jacket and tube contains inert helium gas at slightly above atmospheric pressure. Maximum temperatures of approximately 850°F could occur somewhere within the ETR and ATR tube walls. It can be seen that the operating conditions for both the ETR and ATR tubes are quite similar. Peak fluxes of 3.3×10^{14} n/cm^2-sec (>1 Mev) for ETR and 1.75×10^{14} n/cm^2-sec. for ATR are also reasonably similar and not expected to influence results.

The in-pile tubes are stressed by internal pressure. Assuming a thin walled tube solution, the longitudinal stress (σ_L) is

$$\sigma_L = \frac{PR}{2t} = 5900 \text{ psi} \quad (1)$$

where P = pressure, 2250 psi
R = tube radius, 1.0625 in
t = wall thickness, 0.2025 in

and the hoop stress (σ_H) is

$$\sigma_H = \frac{PR}{t} = 11{,}800 \text{ psi} \quad (2)$$

Thus, the IPT's, while in service, are constantly exposed to a principal hoop stress of 11,800 psi at approximately 700°F. A higher stress, 15,500 psi, occurs in brief excursions for leak tests.

B. Previous IPT Lifetime Extension Studies

Previous IPT lifetime extension justifications were based on data from the literature (Refs. (1-3)) or burst test data. Published literature on Types 347/348 stainless steel have been based on specimens made directly from expended tubes (Ref. (2)) and specimens which were irradiated while stored within the tube, Refs. (1 and 3). Types of data should be distinguished since the prototypic material was irradiated while under a state of stress, a condition which could influence results, although to what extent has not yet been determined. Tensile data from the literature give a preliminary indication of constant or saturated irradiation damage by leveling off of the yield and ultimate strength after initial increases. However, data are limited at higher test temperatures and are nonexistent at fluences approaching the level seen by the material described in this report. A further limitation with some data is due to differing irradiation temperatures which influence the results. It should be noted that fluence values are often reported in n/cm^2 (>0.1 Mev). To compare with the

fluences (E > 1 Mev) used in this work, fluences with E > 0.1 Mev were divided by the factor 1.92, a Bettis estimate.

Brittle fracture of highly irradiated IPT's is a major concern. Longitudinally notched burst test results were used to provide plane strain fracture toughness K_{IC} data. From the semi-infinite plate solution, K_{IC} values were calculated for a part-through crack normal to the hoop stress in the tube (Ref. (4)).

$$K_{IC} = \frac{1.1 \sqrt{\pi a} \ \sigma_f(t)}{\left[1-0.212\left(\frac{\sigma_f(t)}{\sigma_{ys}}\right)^2\right]^{\frac{1}{2}}} \qquad (3)$$

where, $\sigma_f(t)$ = nominal (unperturbed) hoop stress at failure
a = crack depth
σ_{ys} = yield stress

and the half-length of the defect on the surface is assumed to be much greater than a. Such K_{IC} values were then used to compare with a leak-before-break criterion, according to which, a tube can sustain a through-wall crack at the operating load without danger of catastrophic failure provided K_{IC} is greater than that defined by the criterion

$$K = \frac{\sqrt{\pi a} \ \sigma(t)}{\left[1-0.5\left(\frac{\sigma(t)}{\sigma_{ys}}\right)^2\right]^{\frac{1}{2}}} \qquad (4)$$

where $\sigma(t)$ = nominal (unperturbed) hoop stress = $\frac{PR}{2t}$
a = ½ the crack length

Using this formula, assuming a pressure of 3750 psi (ATR operates at 2200 psi), a mean tube diameter of 2.3225 in, a wall thickness of 0.2 in, a crack length twice the wall thickness, and $\sigma(t) \ll \sigma_{ys}$,

$$K = \sqrt{.2\pi}\left(\frac{2.3225}{2(.2)}\right)(3.750) = 17 \text{ ksi}\sqrt{\text{in}} \ .$$

A similar value, 22.6 ksi$\sqrt{\text{in}}$, was estimated based on a criterion for crack arrest toughness using dynamic fracture toughness values which are more conservative than static values and simulate high strain rates typical of a running crack or explosive failure.

Previous fluence extensions were based on burst data resulting in K_{IC} values greater than the failure criterion. However, the extent of irradiation damage a tube might withstand before becoming brittle is uncertain. Further, embrittlement effects at elevated temperatures were even less known, particularly after long exposures at temperature and stress (the in-service conditions of the tube). Although embrittlement is known to occur at high temperatures (>1000°F), the possibilities of its occurring at lower temperatures after exposure to very high fluences had not been studied.

C. Test Objectives

Four types of tests were used in this work.

1. Tensile tests were performed to define the strength properties as a function of fluence. Thus, any loss of ductility for the peak fluence and/or different irradiation temperatures could be determined. Also, elevated temperature testing was performed to determine the strength properties beyond the in-service temperature range and for a base with which to compare delayed rupture tests.

2. Smooth specimen fatigue tests were performed at room temperature to assess any changes in fatigue properties caused by irradiation.

3. Fracture toughness tests at room temperature were performed on notched fatigue precracked specimens to determine brittle fracture properties in the IPT material. In addition, elevated temperature testing was performed to further study embrittlement in the presence of a notch at and beyond service temperatures. Dynamic tests at 800°F were run to simulate high strain rates typical of a running crack or explosive failure.

4. Delayed failure constant stress rupture tests were run to investigate the time dependent effects of embrittlement. Smooth tensile tests were used to check on the possible decrease in steady state creep and premature tertiary failure. Notched and precracked specimens were tested to study crack growth and notch sensitivity.

III. Experimental Procedure

A. Material

The IPT from the H-10 position (Serial Number K-17) was removed from ETR in 1972 and was used in this investigation. The tube was fabricated from consumable electrode vacuum melted, composition Type 347 stainless steel, condition A, in accordance with MIL-S-23195 and certified equivalent to ASME Code A-276 Boiler Code Case 1310 from material per ASTM A182-61.

The ingot was hot rolled with final annealing at 1800°F for 3 hours and water quenched. The room temperature properties were: (1) tensile yield 38.4 to 45.6 ksi; (2) ultimate 85.1 to 89.1 ksi, (3) percent elongation 60.0 to 62.0, (4) percent reduction-in-area 77.5 to 78.5, and (5) hardness R_B 82/83. The hot tensile properties at 800°F were: (1) yield 30.0 to 34.9 ksi, (2) ultimate 55.0 to 56.3 ksi, (3) percent elongation 29.6 to 37.0, and (4) percent reduction-in-area 77.3 to 81.0. The chemical composition of the H-10 IPT is given in Table I.

After removal from service, the H-10 IPT was inspected and sectioned into cylinders approximately four inches high (see Figure 2). Visual and dye penetrant examination for cracking or other defects showed the tube in good condition with no evidence of cracking. Specimens were machined from the sectioned cylinders to one of the two configurations used for testing in this work, tensile and fatigue specimens (Figure 3) and fracture toughness specimens (Figure 4). Each four-inch cylinder was slit parallel to the tube axis to yield six specimens

as shown in Figure 5. The sectioned cylinder coded specimens and respective specimen configurations used for this work are listed in Table II. Included in this table are the fluence data used to arrive at the fluence values reported for this work. Differences in the fluence data are partly due to different correction factors applied to the radiochemical analyses used in the calculation of the fluence. Thus, averages of the different reported results were used. It should be noted that flux wire monitor readings at three radial peak positions showed a fluence range from 3.55 to 4.04 x 10^{22} n/cm^2 (>1 Mev). Therefore, a specimen to specimen variation of $\pm$ 0.25 x 10^{22} n/cm^2 (>1 Mev) is not unlikely. The fluence and irradiation temperatures are also included on Figure 2. The irradiation temperatures of the cold segments were not determined, but were assumed to be slightly higher than the water temperature, 550°F.

B. In-Cell Mechanical Test Machine

An MTS Systems Corporation Model 850 Structure Test System closed-loop electrohydraulic unit with a 50,000 lb. capacity was used for the mechanical testing. The system was equipped with a dual trace storage oscilloscope, X-Y recorder, and environmental chamber capable of temperatures above 1000°F and accurate to approximately $\pm$ 2°F. The load frame, actuator, and environmental chamber were fixed in-cell in the Bettis Hot Laboratory. The hydraulic pump and instrument console were located out-of-cell for remote operation. Specially designed pinned adaptors were used to load the specimens.

C. Tensile Testing

Tensile testing of specimens machined as shown in Figure 3 was performed at room temperature, 600°F, 800°F, and 1000°F. The testing was conducted at a displacement rate of 0.05 inches per minute and stress-strain curves were recorded on the X-Y recorder by using a water-cooled, high-temperature extensometer manufactured by MTS System Corporation. The measurement precision for yield or ultimate strength was -0.06, +0.34 ksi. For the elevated temperature tests, specimens were held at temperature for at least one-half hour before testing. Pre-test and post-test measurements of the cross sectional areas and gage length were made by measuring scaled photographs taken of the specimens in-cell using a viewing periscope. To account for plastic necking, final areas were determined from the formula

$$A = \frac{h}{3}\ (a + 2d) \qquad (5)$$

where h = width
a = thickness at center
d = average thickness at ends
] in the fracture plane

D. Fatigue Testing

The fatigue tests were performed at room temperature on specimens of the same geometry as the tensile tests (Figure 3). The specimens were cycled under load control conditions in tension-tension loading. Fully reversed, displacement control conditions were desired but precluded for this test because modification of the test set-up was required. The load range was 100 to 3000 lbs., which corresponds to a stress range of 2 to 58 ksi. Frequency was 1 cps to at least 3000 total cycles, then it was increased to 5 cps to speed completion of the test.

E. Fracture Toughness Testing

Single-edge-notched (SEN) specimens, Figure 4, were used in the fracture toughness testing. Fatigue pre-cracking at room temperature was accomplished at 20-30 cycles per second under a cyclic load of 50 lb. up to a maximum of 2000 lb in accordance with ASTM E-399-74. Crack growth was monitored by an attached clip-on displacement gage and by viewing and measuring the crack from outside the cell with a transit. Final crack lengths were determined from post-test photographs of the fractured surfaces according to ASTM E-399-74. The fracture toughness tests were also performed basically in accordance with ASTM E-399-74. Two modes of testing were studied. Static fracture toughness tests were made using the standard ASTM E-399-74 recommended loading rate of 30-150 ksi $\sqrt{\text{in.}}$/minute and recording the load-displacement curve on the X-Y recorder in a manner similar to the tensile tests. High rate dynamic testing was also performed on selected specimens. These test specimens were loaded in stroke control at the highest rate attainable by the machine, approximately 3×10^5 ksi $\sqrt{\text{in.}}$/minute. Load and displacement were both monitored versus a time base using the dual trace storage oscilloscope. For the room temperature fracture toughness tests a commercial double cantilever clip-on displacement gage was used. For the elevated temperature tests, a special displacement gage, employing welded strain gages, was designed and fabricated by Westinghouse Research Laboratories (Figure 6). The cantilever beams were lengthened to reduce flexure stress and were made from NiCrFe Alloy X-750 for improved creep resistance. As with the elevated temperature tensile tests, the elevated temperature test specimens were equilibrated for at least one-half hour before testing.

All fracture toughness stress intensity calculations were made using the ASTM E-399-74 95 percent secant intercept method for obtaining the load, P. The standard stress intensity equation for uniaxially loaded SEN specimens was used to calculate the stress intensity as follows (Ref. (5)):

$$K = \frac{P\sqrt{a}}{BW} Y\left(\frac{a}{w}\right) \tag{6}$$

where K = stress intensity
P = load
B = specimen thickness
W = specimen width
a = length of notch plus precrack

and $Y\left(\frac{a}{w}\right) = 1.99 - 0.41\,(a/w) + 18.70\,(a/w)^2 - 38.48\,(a/w)^3 + 53.85\,(a/w)^4$

F. Stress Rupture Testing

Specimens of both the tensile and fracture toughness (notched) geometries were used for the delayed failure stress rupture testing. The notched specimens were pre-cracked as with the fracture toughness testing to test sensitivity to a crack-like defect. The tensile specimens were tested to better characterize the creep properties.

Tests were performed by first loading the specimens in air at temperature (600°F, 800°F, or 1000°F) to 90 percent of the test temperature yield strength as determined from tensile tests, and holding for 100 hours. The test machine was equipped with an automatic triggering feature which shut the machine off in the event of a specimen failure while recording the time of occurrence. If the specimen survived the 100 hours, the specimen was then loaded to 95 percent of the yield strength and tested for an additional 100 hours before pulling the specimen to failure.

G. Density Measurements

Density measurements were made on selected high fluence specimens by an immersion technique using a Mettler balance with an accuracy of ± 0.0002 gm.

H. Summary

A total of 53 mechanical tests (22 tensile, 3 fatigue, 19 fracture toughness, and 9 stress rupture tests), were performed for this work. A schedule of specimens tested is shown in Table III.

IV. Results and Discussion

A. Tensile Properties

A tabulation of the irradiated Type 347 stainless steel tensile properties determined in this work at their respective fluence levels and irradiation and test temperatures appears in Table IV. A comparison of the low fluence, 0.0004 and .001 x 10^{22} n/cm^2 (>1 Mev), tests at room temperature and 800°F with the values given in Section III.A for the unirradiated tube material shows that irradiation to these fluences caused only slight differences in the mechanical properties. Among the differences were small increases in room temperature and 800°F yield and ultimate strength and somewhat more significant decreases in ductility as exhibited by the reduction in areas. In several instances, the total elongation values for this work, based on final gage length measurements, were unavailable for reasons such as failure outside the gage section or difficulty in reading the scribe marks after testing; and the greater than (>) value reported was that obtained from the extensometer, which had a range of 0-150 mils.

At higher fluence levels, 2-4 x 10^{22} n/cm^2 (>1 Mev), the changes in mechanical properties are much larger, which was expected based on previous studies (Refs. 1-3). The yield strengths are increased by a factor of about three, while the ultimate tensile strengths are almost doubled. More significant is the fact that at the higher fluence levels at all of the respective test temperatures the ratios of σys/ σuts approach a value of unity as compared to the value of 0.5 in the unirradiated and lower fluence materials. In conjunction with the convergence of σys and σuts, the uniform elongation decreases considerably, in some instances (at elevated temperatures) to values of less than 1%. Although previous embrittlement criteria have limited uniform elongation to a 1% minimum, a permissible decrease below this limit is reasonable from a tensile stress standpoint, since the yield stress is greatly increased for the irradiated material. The increased yield stress provides an elastic strain range of even greater magnitude proportional to the in-service stress levels of the IPT. (Based on qualitative observations, the modulus of elasticity tended

to decrease with increased irradiation providing even more elastic strain.) A better evaluation of brittle fracture behavior is provided by the fracture toughness tests, which revealed more conclusively that the material was not brittle.

The effects of test temperature on the 0.2% offset yield and ultimate tensile strength for high fluence, low fluence, and the unirradiated material are shown in Figure 7. The values for the highly irradiated material indicate no unexpected changes due to irradiation. The high fluence values at 1000°F show a more rapid decrease in magnitude, whereas the low fluence and unirradiated values remain nearly linear with increasing temperature. However, since the initial values in the highly irradiated case are so much larger, the more rapid decrease in properties is not surprising since it is reasonable to assume that some relaxation or softening resulting from the 1000°F test temperature may occur.

A plot of the room temperature 0.2% offset yield and ultimate tensile strength versus fluence for the Type 347 stainless steel IPT specimens is shown in Figure 8. Included on the plot are data from other studies, Refs. (1-3), for comparison. In addition to the best fit curves for the data of this work, curves are drawn through the data of Kangalaski, et al (Ref. (1)), to emphasize the saturation level which was suggested at increasing fluence levels. The data of this Bettis study also exhibit a similar saturation occurring at a higher stress level, 140 ksi as compared to 110 ksi. A potential reason for the higher saturation stress levels is the higher irradiation temperatures of the H-10 tube. The other values included on the plot, Refs. (2) and (3), illustrate the increase in stress level exhibited with increasing irradiation temperature. It should be noted that the irradiation temperatures of the H-10 IPT varied and were higher at the higher fluence regions of the tube. In the mean temperature range considered, 550-703°F, based on the other data included on the figure, the bias in the shape of the curve caused by the varying temperature was not expected to be large. For purposes of lifetime extension justification, the varying irradiation temperature curve is ideal, since it is prototypic of the in-service conditions. Observing the highest fluence level tested, 3.98×10^{22} n/cm^2 (>1 Mev), which is also the highest irradiation temperature, no indications of annealing of the irradiation damage, typically resulting in decreased yield and tensile strengths (Ref. (2)), were exhibited.

In Figures 9-11, the hot tensile properties, 0.2% offset yield strength and tensile strength, are plotted for 600°F, 800°F, and 1000°F, respectively. Where available, data from other studies are included for comparison. As in the room temperature case, the data show saturation and leveling off of properties with no indications of embrittlement or higher irradiation temperature annealing.

The room temperature and elevated temperature tensile properties determined in this work indicate irradiation of Type 347 stainless steel to 4×10^{22} n/cm^2 (>1 Mev) causes no degradation of properties such as loss of strength or brittleness. The fractured surfaces, Figure 12, of the room temperature test specimens exhibited typical cup-and-cone or ductile type fractures. Fracture surfaces of the elevated temperature tests appeared similar, except for the 1000°F tests, which displayed a dark oxide layer as expected. The fracture strengths were typical of those determined in other studies (Ref. (2)). From room temperature

to temperatures well above the normal ATR operating range, the damage appears to be saturating out as indicated by the leveling off of tensile properties. Since Ref. (2) results at much lower fluence levels (approximately 1 to 6 x 10^{21} n/cm^2 (>1 Mev)) were similar to those of this study up to 4 x 10^{22} n/cm^2 (>1 Mev), significant changes in the tensile properties at levels even above 4 x 10^{22} n/cm^2 (>1 Mev) are not expected.

B. Fatigue Properties

The unnotched fatigue specimen test results at room temperature are presented in Table V. All three specimens tested failed from crack initiation at the hole in the specimen end where the specimens were pinned to the grips. This occurrence may be attributed to stress concentrations caused by either the hole itself, non-axisymmetric loading, or machining marks which were observed in some instances in this location. Since failures occurred at such stress concentrations, it is obvious that the results obtained are conservative, since the gage section undoubtedly could have withstood additional cycles. It should be noted that in none of the tests was a crack detected prior to failure. Thus, it was presumed that failure occurred shortly after crack initiation.

The cyclic stress level used for the fatigue tests, 56 ksi, is significantly greater than the maximum stress range of 15.5 ksi experienced by the ATR IPT's. Further, the design values of the total number of pressure and thermal cycles over the full life of the IPT's are 500 and 900 respectively, or a total of 1400 cycles. The cycle to failure values obtained in this work are well in excess of the total design fatigue life.

Kangilaski, et al (Ref. (1)), have studied the fatigue properties of Type 347 stainless steel irradiated up to 1.6 x 10^{22} n/cm^2 (>1 Mev) at 122°F and tested at room temperature. One of their findings was that irradiation increased the stress necessary for fracture at a given number of fatigue cycles. This result is consistent with the failure of the low fluence, HX2 specimen, which was stressed to the same stress level as the higher fluence specimens, and which failed in a lower number of cycles. Kangilaski, et al also found that fatigue life increased or stayed the same after irradiation for total strain ranges of less than 1.3 percent. In this work the stress level of 56 ksi corresponds to a total strain of $\Delta\epsilon_t = \Delta\sigma/E = 56{,}000/29 \times 10^6 = 0.0019$ at room temperature and similarly $\Delta\epsilon_t = 56{,}000/24 \times 10^6 = .0023$ at 800°F. The decrease in the total number of cycles to failure for the highest fluence specimen was probably due to statistical error which was intensified by the stress concentrations. However, as previously discussed, both values are well above the design requirements and exhibit no degradation due to the higher irradiation temperatures of this work.

Using the Universal Slopes Equation to relate tensile properties to fatigue life for irradiated material (Ref. (6)),

$$\Delta\epsilon_t = \frac{3.5\ \sigma_{uts}}{E} N_f^{-0.12} + D^{0.6} N_f^{-0.6} \qquad (7)$$

where $\Delta\epsilon_t$ = total strain range
σ_{uts} = ultimate strength
E = Young's modulus
D = fracture ductility = ln (100/(100 - RA))
RA = reduction in area, percent
N_f = cycles to failure

predicted N_f values are compared with experimental values in Table VI. The predicted values were calculated using twice the total strain for conservatism. As can be seen, the predicted values are considerably higher. The table also shows that predicted fatigue life values in the ATR service temperature range of approximately 800°F are also high. Using the universal slopes method of lifetime prediction, based on the tensile properties obtained in this work, fatigue should be adequate at large fluences. Although the experimental values obtained were less than predicted, these values display no grossly derogatory effects which might indicate that irradiation was causing some departure from the normally predicted fatigue life, especially since failures did not occur in the gage section. Since the fatigue life at a stress range considerably higher than the in-service stress range was found to be between one and two orders of magnitude larger than the design values, there are no apparent reasons why ATR lifetime extension cannot be justified from a fatigue standpoint.

C. Fracture Toughness Properties

The fracture toughness test values for the irradiated Type 347 stainless steel IPT material were relatively high and indicative of ductile material. These results are given in Tables VII and VIII for the static and dynamic tests, respectively, and are also shown graphically on Figure 13. Oscilloscope trace photographs of two of the dynamic fracture toughness tests are included in Figures 14 and 15 to illustrate the technique used for performing these tests. The load trace of specimen HD5 went off scale before returning to its baseline value. The load range was therefore doubled for subsequent tests. The sawtooth righthand portions of the oscilloscope traces are simply baseline electronic noise and/or clip-on displacement gage shock vibrations after specimen failure. Load value for specimen HD5 was obtained from an electronic backup memory unit. As can be seen, the general trend was that the fracture toughness values increased with increasing fluence at all temperatures, thus indicating improved resistance to fracture from a crack-like defect.

The values which were obtained at the fluence levels of 2.95 and 3.44 x 10^{22} n/cm^2 (>1 Mev) all were over three times the minimum required value of 17 ksi $\sqrt{in.}$ predicted from the leak before break criterion. Alternately, in terms of margin on crack length, the ratio would be increased from three to nine.

As an alternative approach, a minimum dynamic fracture toughness value can be estimated using the ASME Boiler and Pressure Vessel Code Article A-3000, Section XI 1974 edition for a part-through crack as follows:

$$K_I = \sigma_m M_m \left(\frac{\pi a}{Q}\right)^{\frac{1}{2}} + \sigma_b M_b \left(\frac{\pi a}{Q}\right)^{\frac{1}{2}} \qquad (8)$$

where σ_m, σ_b = Membrane and bending stresses
a = Minor half-diameter of embedded flaw or flaw depth for surface flaw = 1/2 thickness, $\frac{t}{2}$
Q = Flaw shape parameter
M_m = Correction factor for membrane stresses
M_b = Correction factor for bending stresses (Critical length - 2t = 0.4 in)

From this equation, a minimum K_I of 23 ksi $\sqrt{in.}$ was obtained. The values obtained for the dynamic fracture toughness in this study were again all greater than three times this minimum. Even at the highest fluence, 3.44 x 10^{22} n/cm^2 (>1 Mev), the value for the dynamic fracture toughness remained high with no indications of brittleness.

The fracture surfaces of most of the static and dynamic tests displayed shear lips typical of ductile fracture (See Figure 16). Several specimens even displayed full oblique fracture appearance. The fatigue precracks, however, were observed to be partially skewed in shape in practically all of the specimens, with the crack on the outside region of the tube wall generally larger in length "a" than along the inner surface as shown in Figure 16. This was expected with the curved shaped specimens. Although invalid per ASTM E-399-74, it was judged that reasonable measurements of the crack length could still be obtained from averaging crack-length measurements across the specimen thickness and that the test results would still be meaningful. Also, it should be noted that the orientation of the crack in the specimens was perpendicular to the direction of a crack expected to occur from the maximum hoop stress, i.e., parallel to the axis of the tube. However, this difference is difficult to overcome, since there are no standard fracture toughness specimens which are easily obtained from the cylindrical sections. As in the case of the crack shapes, this difference was not judged to cause loss of meaningful results.

The main concern with validity of results rests with specimen thicknesses. A valid plane strain fracture toughness parameter, K_{IC}, was not reported for these tests because the ASTM criterion for validity regarding specimen thickness, $B > 2.5\left(\frac{K_{IC}}{\sigma_{ys}}\right)^2$, was not met since the specimens were too small. Nevertheless, the values reported are those obtained from measurements on specimens which are prototypic of service conditions in the sense that the specimen thickness is the tube wall thickness. For the specimens tested, with results one might consider as measures of the yield strength more than fracture toughness (due to the undersize specimens and the ductility exhibited), the values are relatively high and are well above the values predicted by the leak-before-break (LBB) criterion on this size region. Thus, since the specimens of this study, with the thickness prototypic of the intended application, exhibited ductile failures, it was concluded that brittle fracture was not a problem for material irradiated to the range of this work. Further, the values generally appear to be increasing with increasing fluence (a trend observed previously for "valid" K_{IC} values for Zircaloy by Walker and Kass (Ref. (7)). However, data are thus far too limited to conclude whether the fracture toughness values will continue to change or will remain constant for further fluence increases. The data do indicate that increasing the loading rate (dynamic tests), and/or increasing the test temperature do not cause any significant changes to the fracture toughness for the fluence levels tested.

D. Stress Rupture Properties

The delayed failure stress rupture test results are listed in Table IX. Several problems were encountered in conducting these tests which resulted in less obtained information than was originally intended. However, several qualitative results were obtained.

The test specimen irradiated to 2.22×10^{22} n/cm^2 (>1 Mev) survived 100 hours at 82% of the yield stress at 600°F and showed no indications of impaired stress rupture properties due to embrittlement from helium transmuted from boron. In addition, specimens irradiated to the lower fluence levels, 0.0001-0.001 x 10^{22} n/cm^2 (>1 Mev), survived either 100 or 200 hours of testing at temperatures ranging from 600 to 1000°F at stresses at or above the respective yield stresses. Since the 1000°F test in particular did not display any evidence of high temperature embrittlement, it becomes even more unlikely that such embrittlement would be a possibility at the IPT service temperatures. Further, since most of the surviving specimens were notched and precracked, no indications of notch sensitivity were detected.

It is worth noting that the specimens which failed were highly stressed indicating that tensile notch sensitivity is not significant. The reason for the failures on loading, and a major problem of the test, was the inability to accurately estimate the cross sectional area remaining in the failure plane after precracking, since, as discussed in the section on fracture toughness, the fatigue cracks were often skewed and approximate measures of the areas could only be made after the specimens were fractured. Hence, in attempting to load the specimens as close to the yield as possible, underestimates of the crack sizes caused premature failures as noted for specimen HH4. For the lower fluence specimens where the ultimate tensile stresses were considerably higher than the yield, failures on loading were not as great a problem, since a larger margin for errors in the crack-size estimates existed.

To avoid the trial and error situation involved with the notched and precracked specimens, two tensile specimens were tested as delayed failure stress rupture tests. Such tests, it was judged, would provide results more comparable with creep data. The low fluence specimen survived 200 hours of testing at 1000°F. Unfortunately, the high fluence specimen HC1 failed at a stress slightly lower than yield stress predicted from the tensile test and no stress rupture information could be obtained. This caused specific stress rupture information at high fluences to remain inconclusive. The low fluence specimen data, however, were sufficient to show that no premature testing creep failures occur due to the low fluence irradiation.

E. Density Measurements

Density measurements from selected high fluence specimens, 3.44-3.98 x 10^{22} n/cm^2 (>1 Mev), were made and compared with the unirradiated material. The results are reported in Table X, which show a volume change of $\Delta V/V$ of .21 to .25%. These results show that only slight swelling may have occurred in the material, but the data are too limited to provide any conclusive correlation to fluence. Thus, these data are presented for information only.

V. Conclusions

Based on the test results described herein, the following conclusions were drawn.

1. Significant increases in the yield and ultimate tensile strengths occur after irradiation to fluences up to approximately 4 x 10^{22} n/cm^2 (>1 Mev). However, such increases occur at lower fluence levels and appear to remain constant, indicating saturation of the irradiation damage.

2. Although the uniform elongation decreases significantly, it also appears to have leveled off to constant values, and the overall ductility as indicated by total elongation and reduction in area remains reasonably good. Further, irradiation results in an increased safety margin from ductile failure because of the increased yield strength of the material.

3. Fatigue properties are satisfactory after irradiation to 4 x 10^{22} n/cm^2 (>1 Mev).

4. The fracture toughness results indicated that the Type 347 stainless steel remained ductile after irradiation to 3.44 x 10^{22} n/cm^2 (>1 Mev) and the fracture toughness values generally appeared to increase with increasing fluence.

5. Dynamic fracture toughness tests resulted in consistently high fracture toughness values and did not display evidence of brittle fracture.

6. No evidence of notch sensitivity or strain rate sensitivity was found in this testing for fluences ranging up to 2.22 x 10^{22} n/cm^2 (>1 Mev).

7. The tensile, fracture toughness, and stress rupture tests displayed good material integrity at all the test temperatures from room temperature to 1000°F.

8. All of the above conclusions indicate that extension of the ATR fluence limit to 4 x 10^{22} n/cm^2 (>1 Mev) is justified with respect to the tests in this study. Further, no reasons to prohibit extension to even higher levels were evidenced.

VI. Acknowledgements

Gratitude is expressed to A. I. Schwartz and F. A. Flint for the useful information provided during the preparation of this report. Acknowledgement is also given to J. F. Hall for advice on the mechanical testing; D. F. Chapas, who performed the tests; and A. Bush of Westinghouse Research Labs, who designed and fabricated the high temperature clip-on displacement gage.

VII. References

(1) M. Kangilaski, F. R. Shober, J. A. DeMastry, and J. E. Gates, "Effects of Large Fast Fluences on Mechanical Properties of Type 347 Stainless Steel and Aluminum," BMI-1834, March 27, 1968.

(2) W. E. Murr and F. R. Shober, "Annealing Studies on Irradiated Type 347 Stainless," BMI-1621, March 6, 1963.

(3) A. E. Powers and E. E. Baldwin, "Effect of Neutron Irradiation in 550°F Loop Water on the Mechanical Properties of Ni-Cr-Fe Alloy 600, Ni-Cr-Fe Weld Metal, and Type 347 Stainless Steel," KAPL-3161, January 27, 1967.

(4) R. E. Johnson, "Fracture Mechanics: A Basis for Brittle Fracture Prevention," WAPD-TM-505, November, 1965.

(5) W. F. Brown, Jr. and J. E. Srawley, "Plane Strain Crack Toughness Testing of High Strength Metallic Materials," ASTM Special Technical Publication No. 410, p. 12, American Society for Testing and Materials, Philadelphia, Pa., 1966.

(6) C. R. Brinkman, G. E. Korth, and J. M. Beeston, "Influence of Irradiation on the Creep/Fatigue Behavior of Several Austenitic Stainless Steels and Incoloy 800 at 700°C," ASTM Special Technical Publication No. 529, pp. 473-490, American Society for Testing and Materials, Philadelphia, Pa., 1974.

(7) T. J. Walker and J. N. Kass, "Variation of Zircaloy Fracture Toughness with Irradiation," ASTM Special Technical Publication No. 551, pp. 328-354, American Society for Testing and Materials, Philadelphia, Pa., 1974.

Table I

Chemical Analysis of the ETR Type 347 Stainless Steel H-10 IPT

Element	Wt. percent
C	0.031
Mn	1.14
P	0.014
S	0.005
Si	0.44
Cr	18.19
Ni	10.97
Mo	0.13
Cu	0.13
Cb + Ta	0.64
Ta	0.02
Co	0.06

Table II

Specimen Designations and Fluence Values

Cylinder Specimen Nos.	Specimen Type*	Irradiation Temperature, °F	Fluences x 10^{22} n/cm^2 (>1 Mev) Orig.(a)	Curve(b)	CPP(c)	Bettis(d)	Avg. (e)	Value Used
HA1-6	1, 2	653	2.30	2.1	-	-	-	2.20 (f)
HC1-6	1	703	4.15	3.8	4.81	3.51	4.16	3.98 (g)
HD1-6	2	703	2.87	3.5	3.30	3.43	3.37	3.44 (g)
HE1-6	1, 2	692	3.44	3.7	3.97	3.22	3.60	3.65 (g)
HG1-6	1, 2	658	3.00	2.9	-	-	-	2.95 (f)
HH1-6	1	628	2.14	2.3	-	-	-	2.22 (f)
HW1-6	1, 2	>550	.001	-	-	-	-	.001
HX1-6	1, 2	>550	.01	-	.01	.06	.03	.02 (h)
HY1-6	2	>550	.0001	-	-	-	-	.0001
HZ1-6	1	>550	.0004	-	-	-	-	.0004

*1 - Tensile or Fatigue 2 - Fracture Toughness

(a) Original Westinghouse and Chemical Processing Plant (CPP)
(b) Best average of (a) and fission rate profile
(c) Adjusted chemical processing plant data
(d) Adjusted Bettis data
(e) Average of (c) and (d)
(f) [(a) + (b)]/2
(g) [(b) + (e)]/2
(h) [(a) + (e)]/2

Table III

Type 347 SS H-10 IPT Specimens Tested

Test emp., °F	Fluence Level	Tensiles	Static Fracture Toughness	Dynamic Fracture Toughness	Fatigue	Stress Rupture
RT	High	HE1, HE2, HC2	HD2, HD3, HD4		HC4	
600		HE3, HC3	HD1			
800		HE4, HE5, HC5	HD6	HD5, HE6		
1000		HC6				HC1
RT	Medium	HH5, HE1	HG2, HA2		HG1	
600		HG5	HG3			HH3, HA1
800		HH6	HG4	HA4, EA5		
1000		HG6, HA6	HH2, HA3			HH4
RT	Cold	HZ1, HZ2	HY2		HX1, HK2	
600		HZ3, HZ4	HY3			HY6, HW2
800		HZ5, HW4	HY4			HW3
1000		HW5	HY5			HW6, HY1

Table IV

Tensile Results

Specimen Number	Fluence $n/cm^2 \times 10^{22}$ (> 1 Mev)	Irradiation Temperature °F	Test Temp., °F	Y.S. (0.2%) ksi	UTS ksi	Fracture Stress, ksi	Uniform Elong. %	Total Elong. %	Reduction in Area
HC2	3.98	703	RT	141.6	146.9	300.0	1.65	26.0	70.8
HC3	3.98	703	600	122.5	123.3	159.2	0.89	5.2	49.8
HC5	3.98	703	800	111.2	111.8	151.3	0.86	> 6.9*	52.9
HC6	3.98	703	1000	87.6	89.5	112.5	1.13	> 10.7*	35.8
HE1	3.65	692	RT	137.9	144.3	287.6	1.5	> 15.0	70.7
HE2	3.65	692	RT	143.0	149.3	312.5	1.5	27.9	72.3
HE3	3.65	692	600	125.4	125.7	138.0	0.62	> 1.4*	37.2
HE4	3.65	692	800	109.2	109.4	103.6	0.80	> 4.9*	35.0
HE5	3.65	692	800	112.0	112.8	125.6	0.65	> 3.0*	35.6
HG5	2.95	658	600	120.2	120.9	151.5	1.2	> 7.4*	49.3
HG6	2.95	658	1000	90.0	91.6	120.3	1.02	> 10.73*	49.2
HH1	2.22	628	RT	140.4	144.7	281.3	1.58	> 15*	68.7
HH5	2.22	628	RT	141.1	145.4	286.6	1.35	> 15*	69.2
HH6	2.22	628	800	108.3	108.8	153.5	0.90	> 10.3*	55.5
HA6	2.20	653	1000	81.3	84.3	124.2	0.90	> 2.6*	52.7
HZ1	.0004	> 550	RT	45.9	87.9	173.4	> 15	> 15	66.2
HZ2	.0004	> 550	RT	48.6	89.3	167.6	> 15	> 15	64.0
HZ3	.0004	> 550	600	39.1	63.5	143.6	> 15	38.0	73.1
HZ4	.0004	> 550	600	34.9	61.3	85.1	> 15	> 15	58.6
HZ5	.0004	> 550	800	32.2	58.1	118.6	> 15	> 15	65.4
HW4	.001	> 550	800	35.7	59.3	134.7	> 15	> 15	70.9
HW5	.001	> 550	1000	36.0	54.1	131.9	> 15	> 15*	73.4

* Broke at or outside gage length

Table V

Fatigue Results

Specimen	Fluence $n/cm^2 \times 10^{22}$ (1 Mev)	Test Temp., °F	Load Range (lb)	Stress Range (ksi)	Frequency Cycles/Sec	# Cycles	Total # Cycles	Comments
HC4	3.98	RT	100-3000	1.94-58.1	1	5000	61,111	Failure in base of
					5	56,110		Speciman at pin hole.
HC1	2.95	RT	100-3000	1.93-57.8	1	10,200	95,110	Failure in base of
					3	85,110		Specimen at pin hole.
HX2	.02	RT	100-3000	1.96-58.8	1	3,000		Failure in base of
					5	23,050	26,050	Specimen at pin hole.

Table VI

Tensile Fatigue Life Calculations for $\Delta\epsilon_t$ = 0.0038 (RT) and 0.0046 (800°F)

Specimen	Fluence $n/cm^2 \times 10^{22}$ (>1 Mev)	Temperature	Tensile Data (This Work) σ_{uts}	Tensile Data (This Work) RA	Approximate N_f(Calc)	N_f (experimental)
HC4	3.98	RT	146.9	70.8	800,000	61,111
		800	111.8	52.9	150,000	-
HG1	2.95	RT	144.7[1]	68.7[1]	700,000	95,110
		800	108.8[1]	55.5[1]	125,000	-
HX2	.02	RT	88.6[2]	65.1[2]	160,000	26,050
		800	59.3[3]	70.9[3]	35,000	-

1 Approximated based on HH ring fluence
2 Approximated based on HZ ring fluence
3 Approximated based on HW ring fluence

Note: E = 29 x 10^6 psi at RT; 24 x 10^6 psi at 800°F

Table VII

Fracture Toughness Results

Static Tests (Loading Rate 30-150 ksi $\sqrt{in.}$/min)

Specimen Number	Fluence $n/cm^2 \times 10^{22}$ (> 1 Mev)	Irradiation Temperature, °F	Test Temperature, °F	Max. Load, lb.	Load, PQ at 5% Secant Offset, lb.	K_Q ksi $\sqrt{in.}$	a/w	Comments
HD2	3.44	703	RT	10,000	7,500	97.5	.25	No precrack
HD3	3.44	703	RT	1,625	1,400	74.5	.67	-
HD4	3.44	703	RT	4,300	3,600	90.0	.50	-
HD1	3.44	703	600	6,370	5,500	81.7	.36	-
HD6	3.44	703	800	6,000	4,500	66.4	.36	-
HG2	2.95	658	RT	6,830	5,850	97.8	.40	-
HG3	2.95	658	600	6,300	5,200	80.1	.37	-
HG4	2.95	658	800	5,610	4,650	74.9	.39	-
HH2	2.22	628	1000	3,400	2,010	46.0	.47	-
HA2	2.20	653	RT	2,800	2,600	81.8	.55	Estimated crack length
HA3	2.20	653	1000	2,070	1,150	30.8	.52	-
HY2	0.0001	550	RT	3,760	1,625	44.3	.53	-
HY3	0.0001	550	600	2,985	975	26.1	.52	-
HY4	0.0001	550	800	2,775	1,425	37.2	.51	-
HY5	0.0001	550	1000	2,565	1,150	30.0	.51	-

Table VIII

Fracture Toughness Results

Dynamic Fracture Toughness Tests (Loading Rate Approx. 3×10^5 ksi $\sqrt{in.}$/min.)

Specimen Number	Fluence $n/cm^2 \times 10^{22}$ (>1 Mev)	Irradiation Temperature, °F	Test Temperature, °F	Max. Load (lb)	Est. Load, P_1 Used to Calc. K_D (lb)	Loading Rate ksi $\sqrt{in.}$/min.	a/w	K_D Ksi $\sqrt{in.}$
HE6	3.65	692	300	6630	6000	3.3×10^5	.37	93.1
HD5	3.44	703	800	>6400	5000	3.7×10^5	.43	91.6
HA4	2.20	653	800	5340	4100	4.6×10^5	.52	117.2
HA5	2.20	653	800	3720	3700	3.5×10^5	.50	94.2

Table IX

Delayed Failure Stress Rupture Test Results

Specimen Number	Fluence $n/cm^2 \times 10^{-22}$ (>1 Mev)	Irradiation Temperature, °F	Test Temperature, °F	First 100 hrs. Actual Stress, Ksi*	First 100 hrs. σ/σ_{ys}	Second 100 hrs. Actual Stress, Ksi*	Second 100 hrs. σ/σ_{ys}	Results
HC1**	3.98	703	1000	78.9	90	-	-	Failed on loading 1st 100 hrs.
HH3	2.22	625	600	96.4	.82	99.0	.83	Failed loading 2nd 100 hrs.
HH4	2.22	625	1000	59.6	.70	-	-	Failed on loading 1st 100 hrs.
HA1	2.20	653	-	-	-	-	-	Failed during pre-cracking (cracked at pinhole)
HY6	0.0001	>550	600	-	-	-	-	Failed on loading 1st 100 hrs.
HW2	0.001	>550	600	51.5	1.40	54.8	1.48	Survived both tests
HW3	0.001	>550	600	54.1	1.51	56.4	1.58	Failed on loading 2nd 100 hrs.
HW6**	0.001	>550	1000	32.4	.90	34.2	.95	Survived both tests
HY1	0.0001	>550	1000	38.8	1.08	41.3	1.15	Survived both tests

* Un-notched specimens - based on load and initial cross sectional areas, Notched specimens - based on load and post test area measurements (area - est. crack area).

** Un-notched

TABLE X

Irradiation Density Change

Sample	Fluence $n/cm^2 x 10^{22}$ (> 1 Mev)	Irradiated Density g/cc	Density Change g/cc	Volume Change Percentage $\Delta V/V\%$
HE1	3.65	7.9194	-0.0196	0.25
HD2	3.44	7.9196	-0.0164	0.21
HC2	3.98	7.9182	-0.0178	0.22

FIGURE 1 - H-10 In-Pile Tube

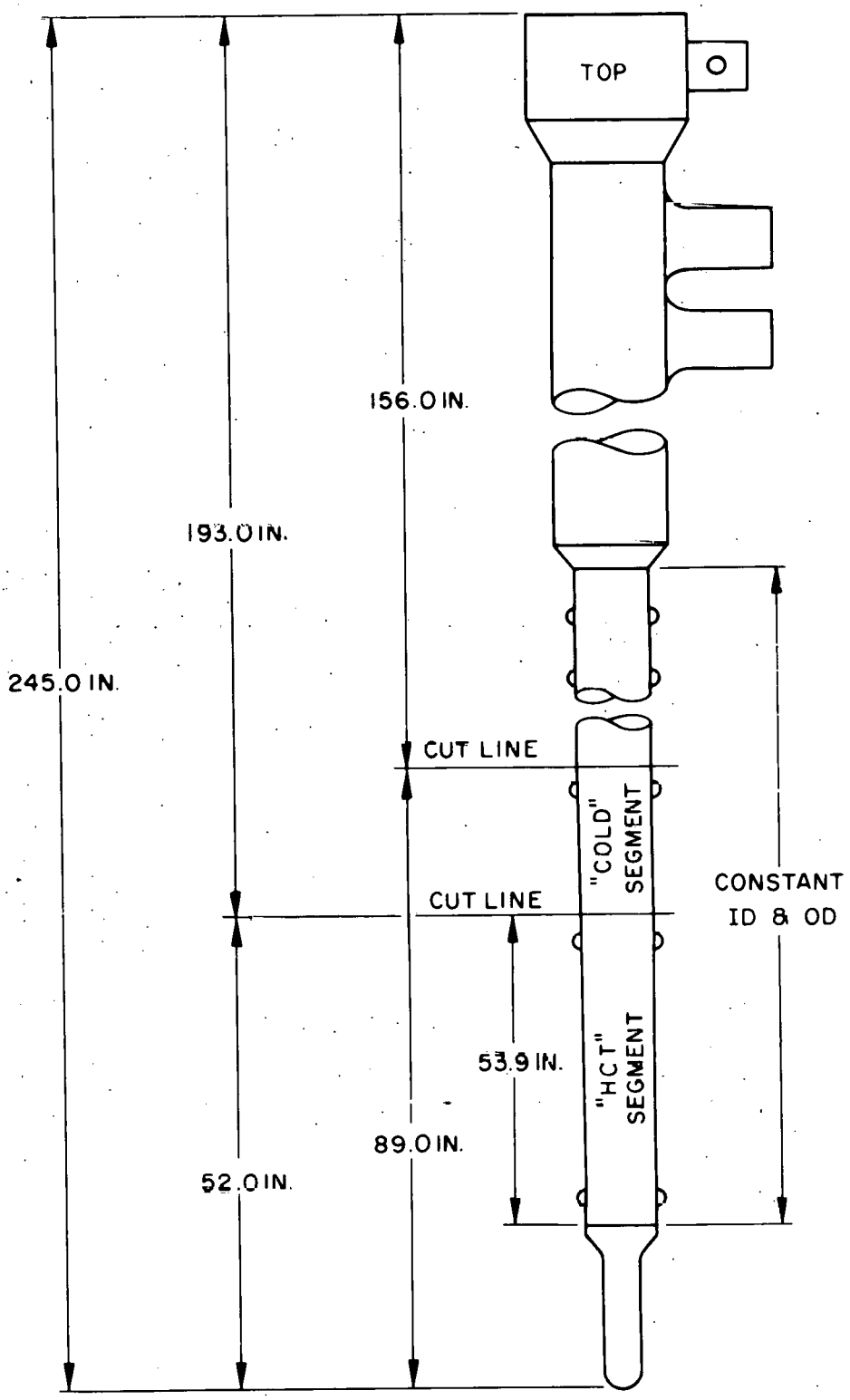

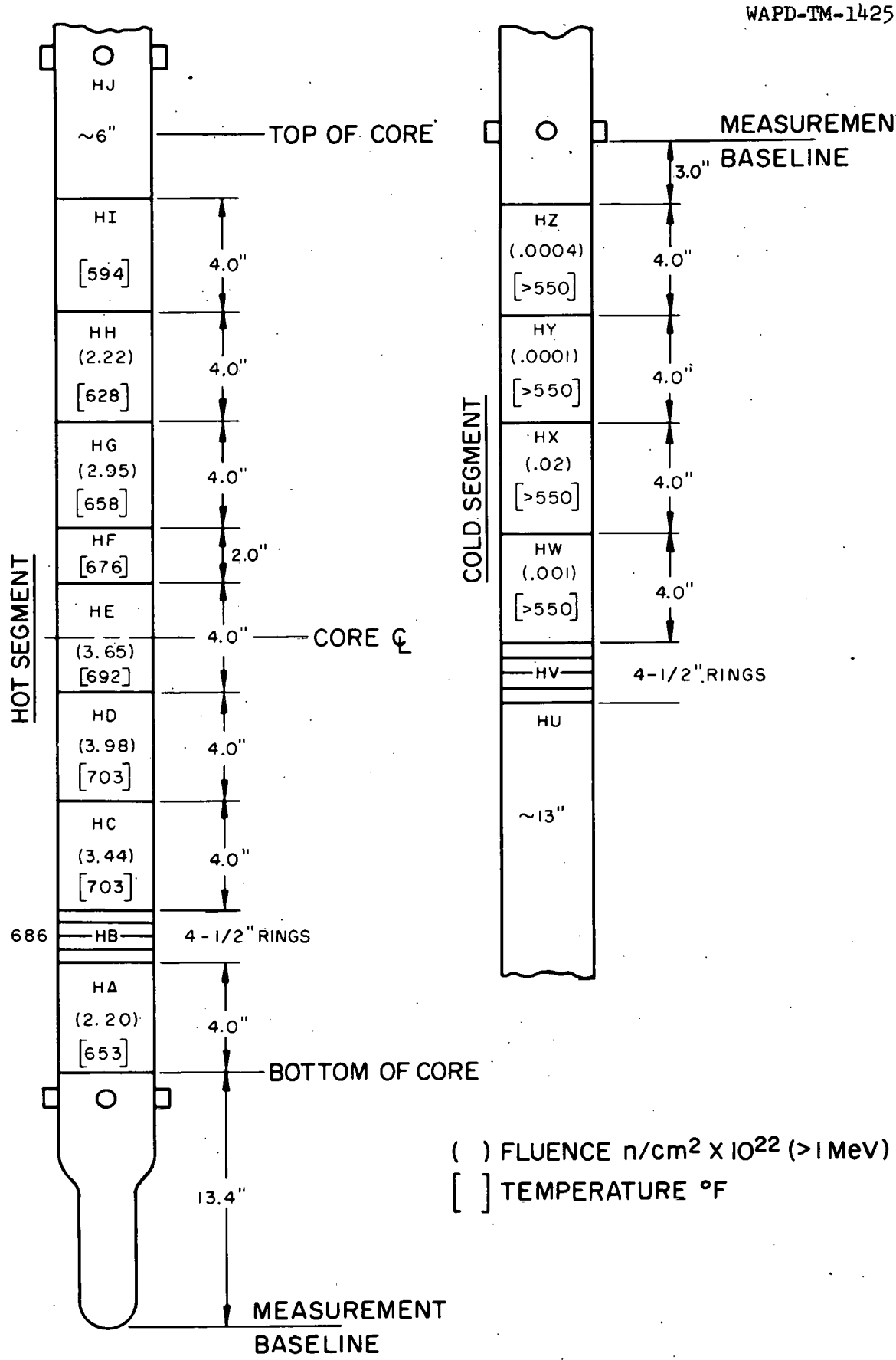

FIGURE 2

Specimen Locations for the ETR H-10 IPT: Hot and Cold Segments

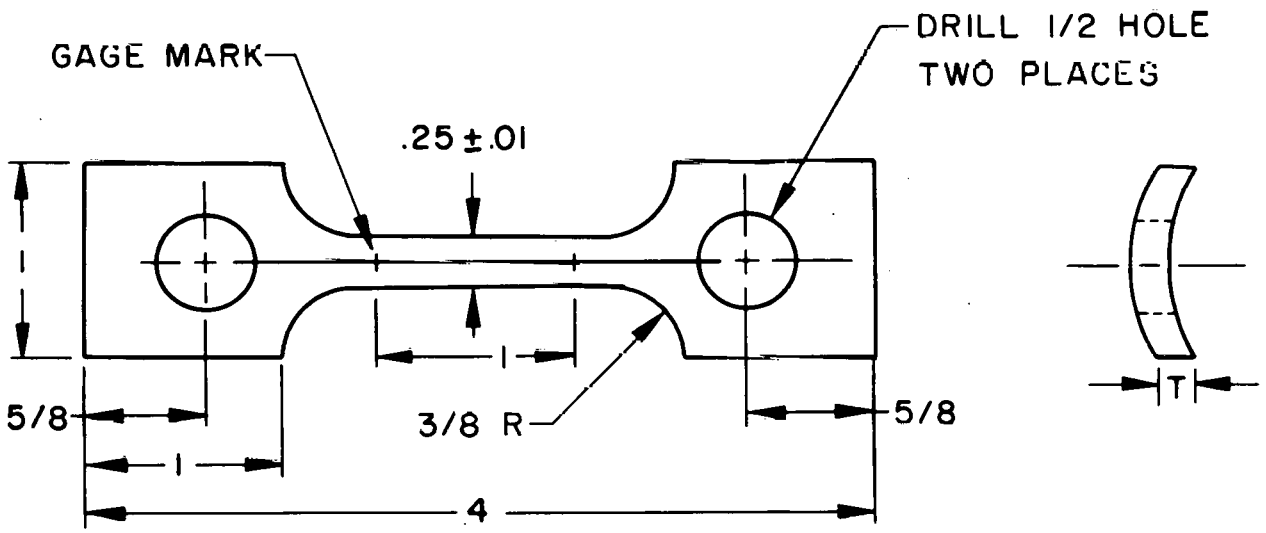

Notes:
1. T equals tube thickness.
2. All dimension in inches.
3. All tolerances ± 1/32 inch except as indicated.
4. Holes must be on centerline of reduced section within ± .002.
5. Gradually taper reduced section toward middle so that middle is not more than .005 inch less than ends of reduced section.
6. Gage marks are to be scribed lightly with dividers or other suitable instruments on the outside diameter.

FIGURE 3 - Tensile and Fatigue Test Specimen

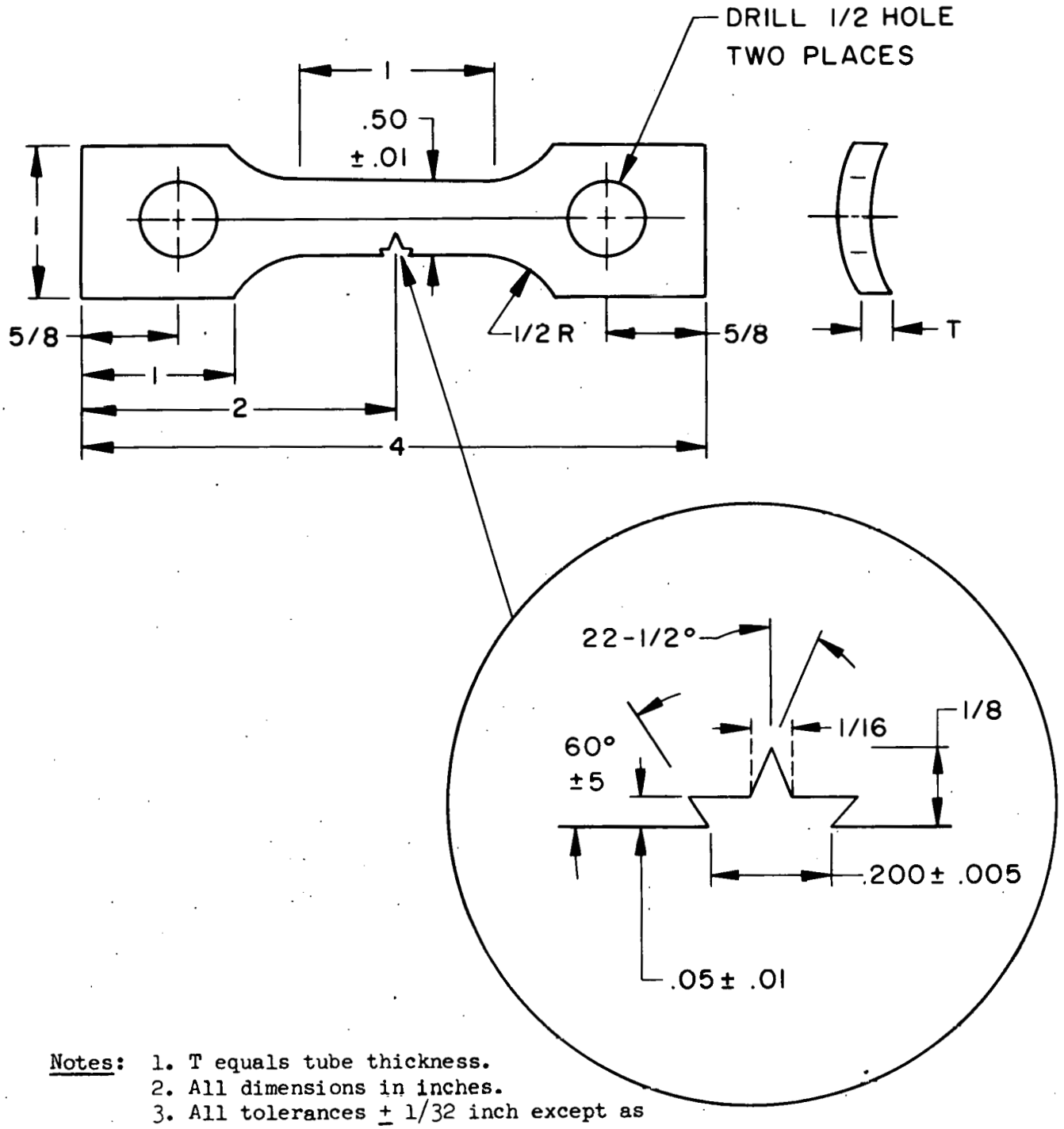

Notes:
1. T equals tube thickness.
2. All dimensions in inches.
3. All tolerances ± 1/32 inch except as indicated.
4. Holes must be on centerline of reduced section within ± .002.
5. Radius at top of notch 0.003-0.005 inches.

FIGURE 4 - Single-Edge-Notched Fracture Toughness Specimen

FIGURE 5
H-10 In-Pile Tube Specimens
Radial Orientation and Identification Location

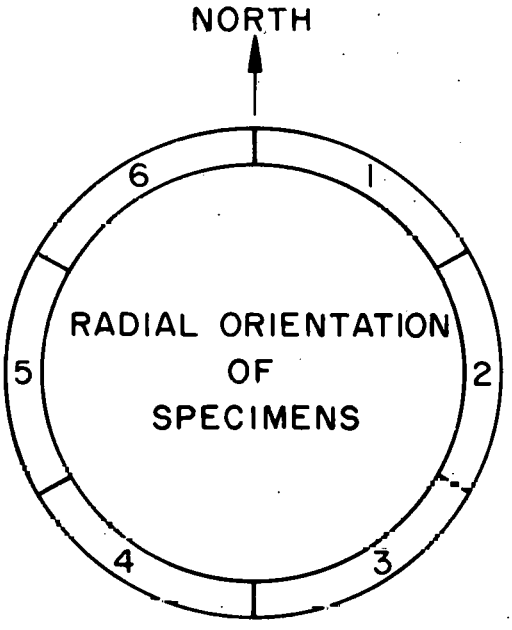

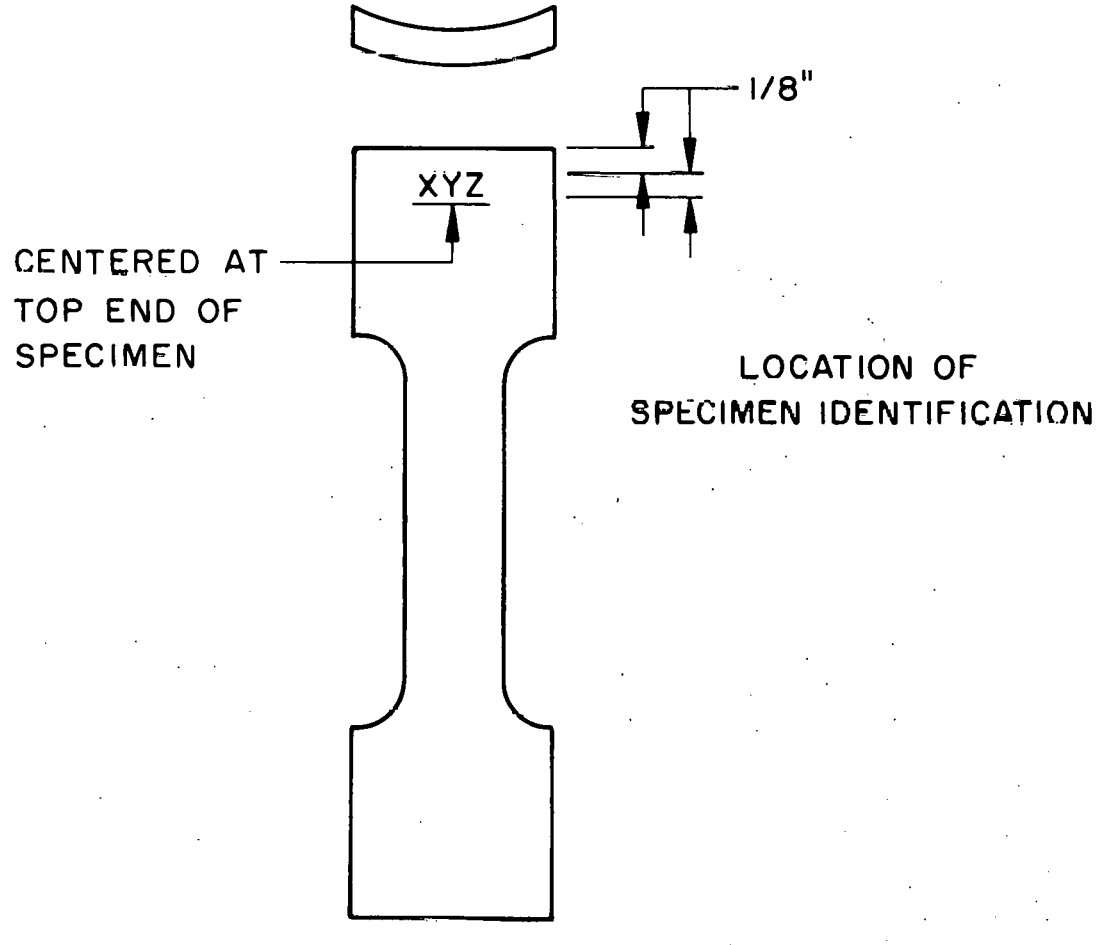

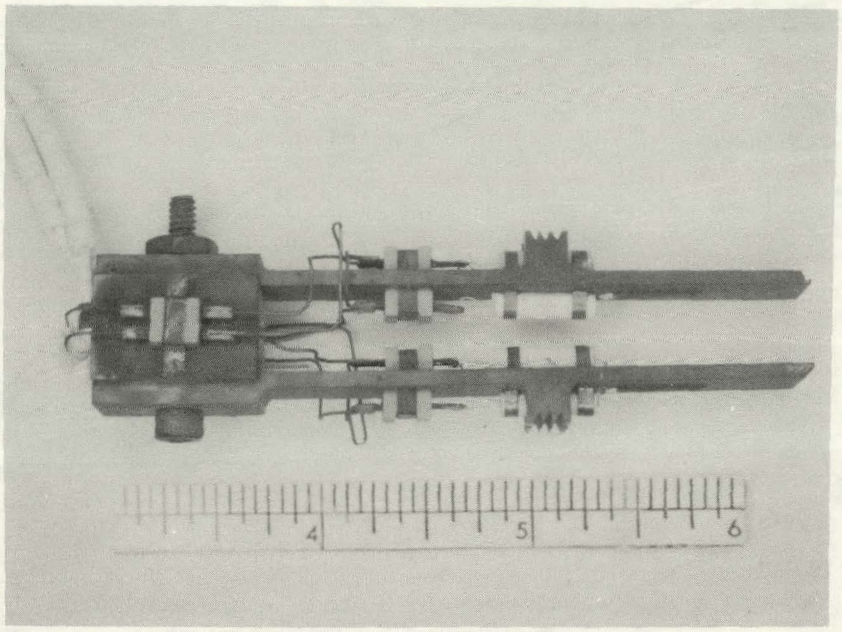

Figure 6 - High Temperature (1000°F) Double Cantilever Clip-On Displacement Gage Designed and Fabricated by Westinghouse Research Laboratories

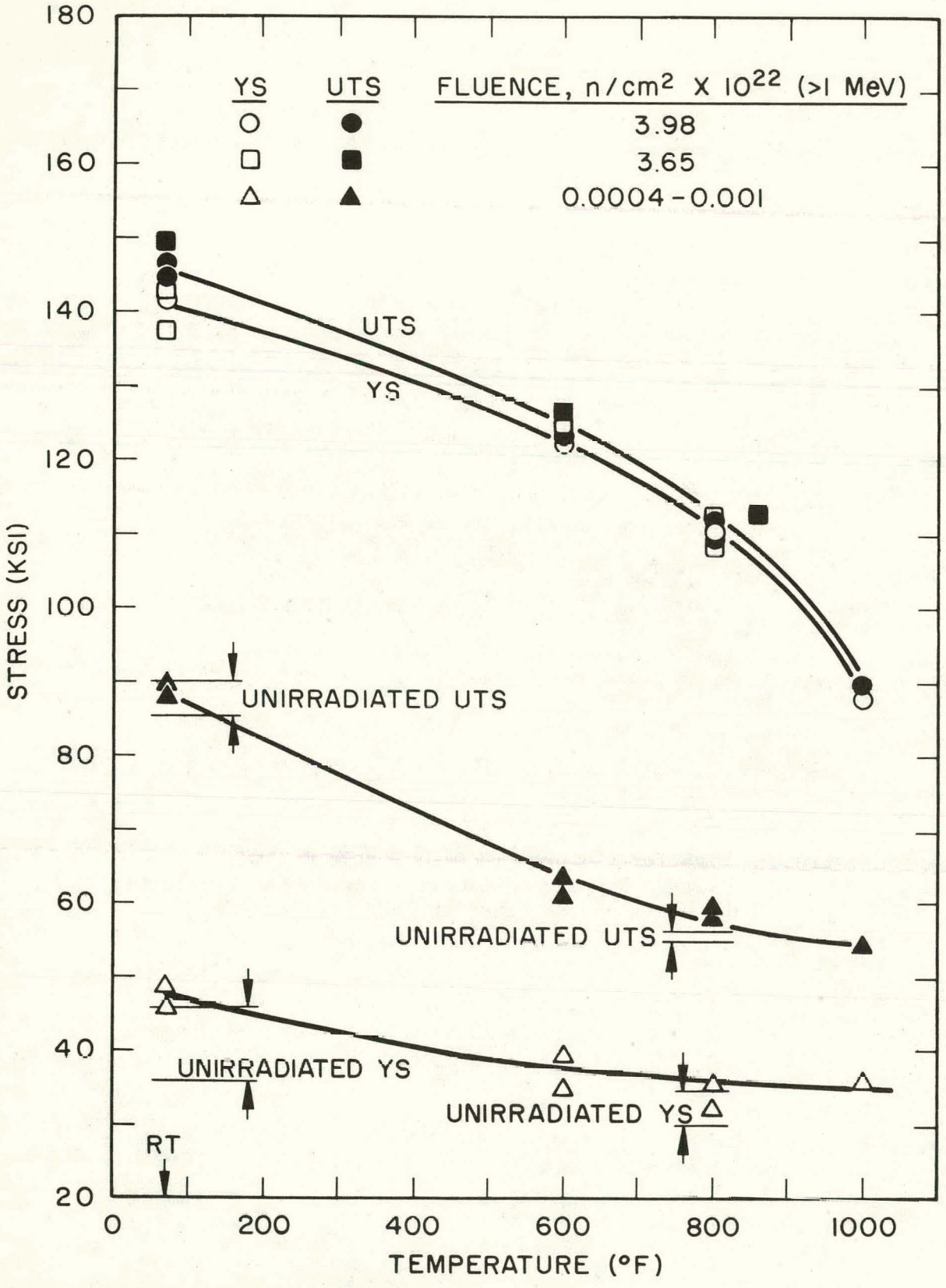

FIGURE 7 - The Effect of Test Temperature on the Tensile Properties of Irradiated Type 347 Stainless Steel

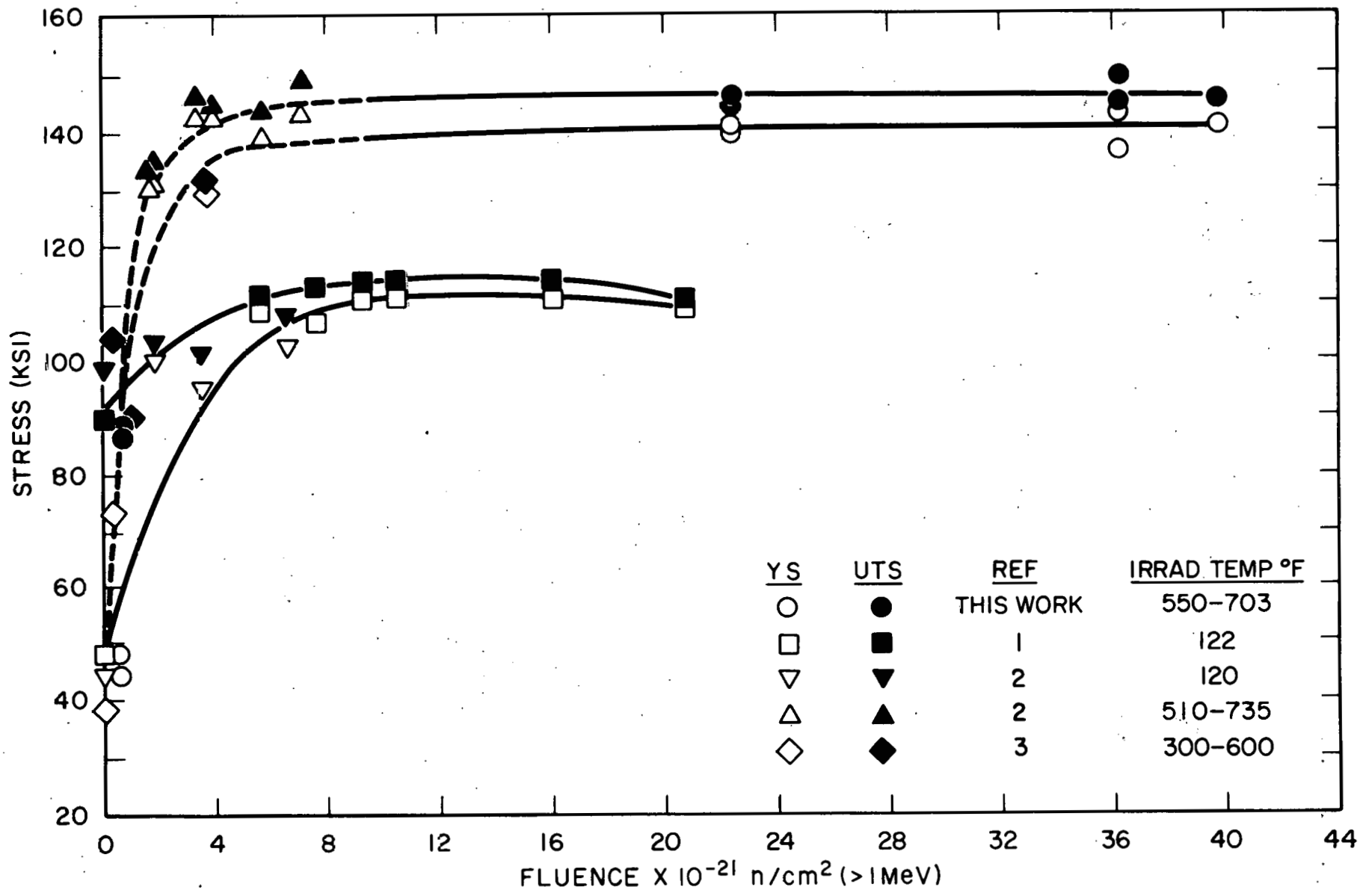

FIGURE 8 - Effect of Fast Fluence on the Room Temperature Yield and Ultimate Tensile Strength of Type 347 Stainless Steel

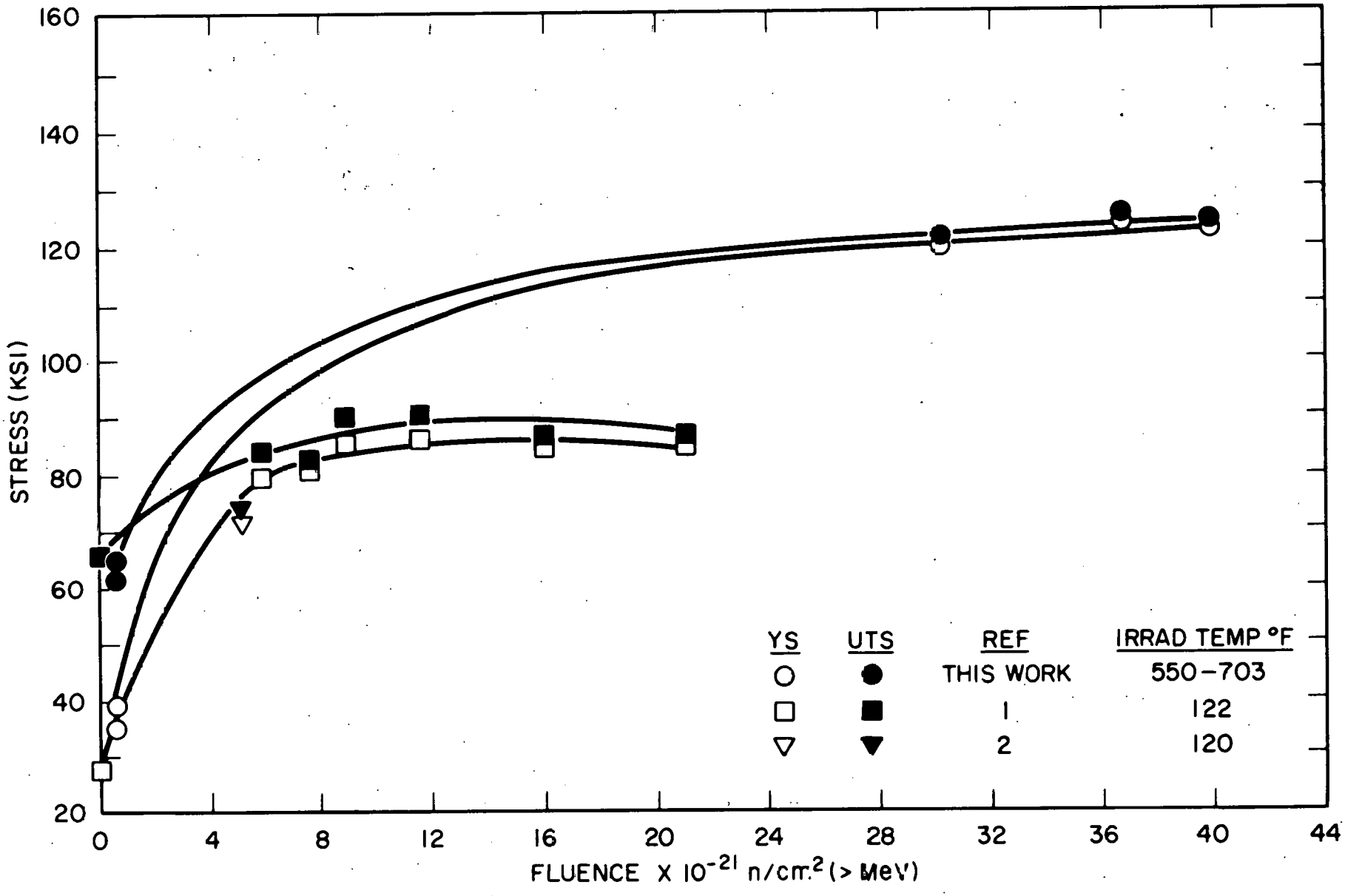

FIGURE 9 - Effect of Fast Fluence on the 600°F Yield and Ultimate Tensile Strength of Type 347 Stainless Steel

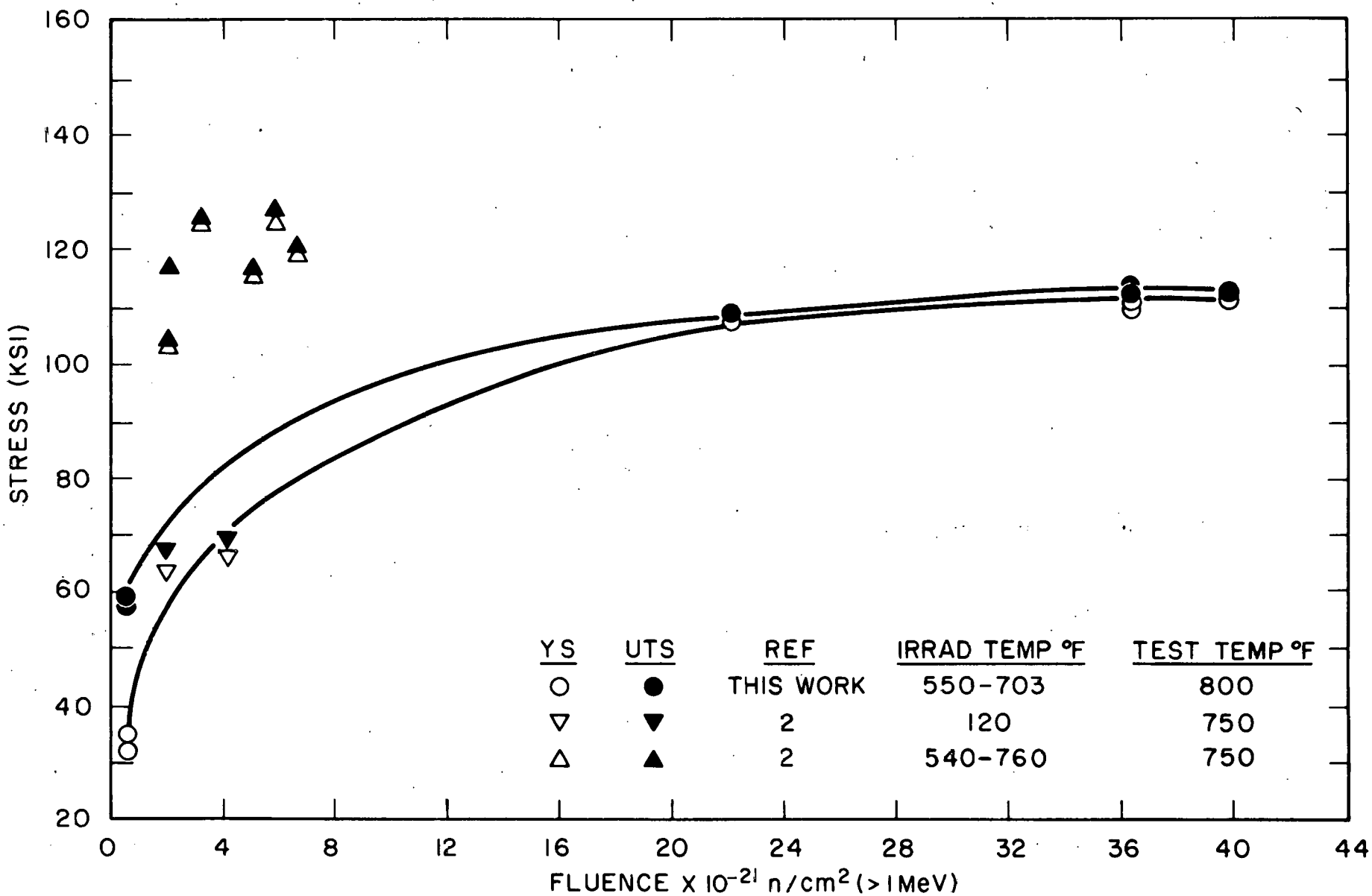

FIGURE 10 - Effect of Fast Fluence on the 750-800°F Yield and Ultimate Tensile Strength of Type 347 Stainless Steel

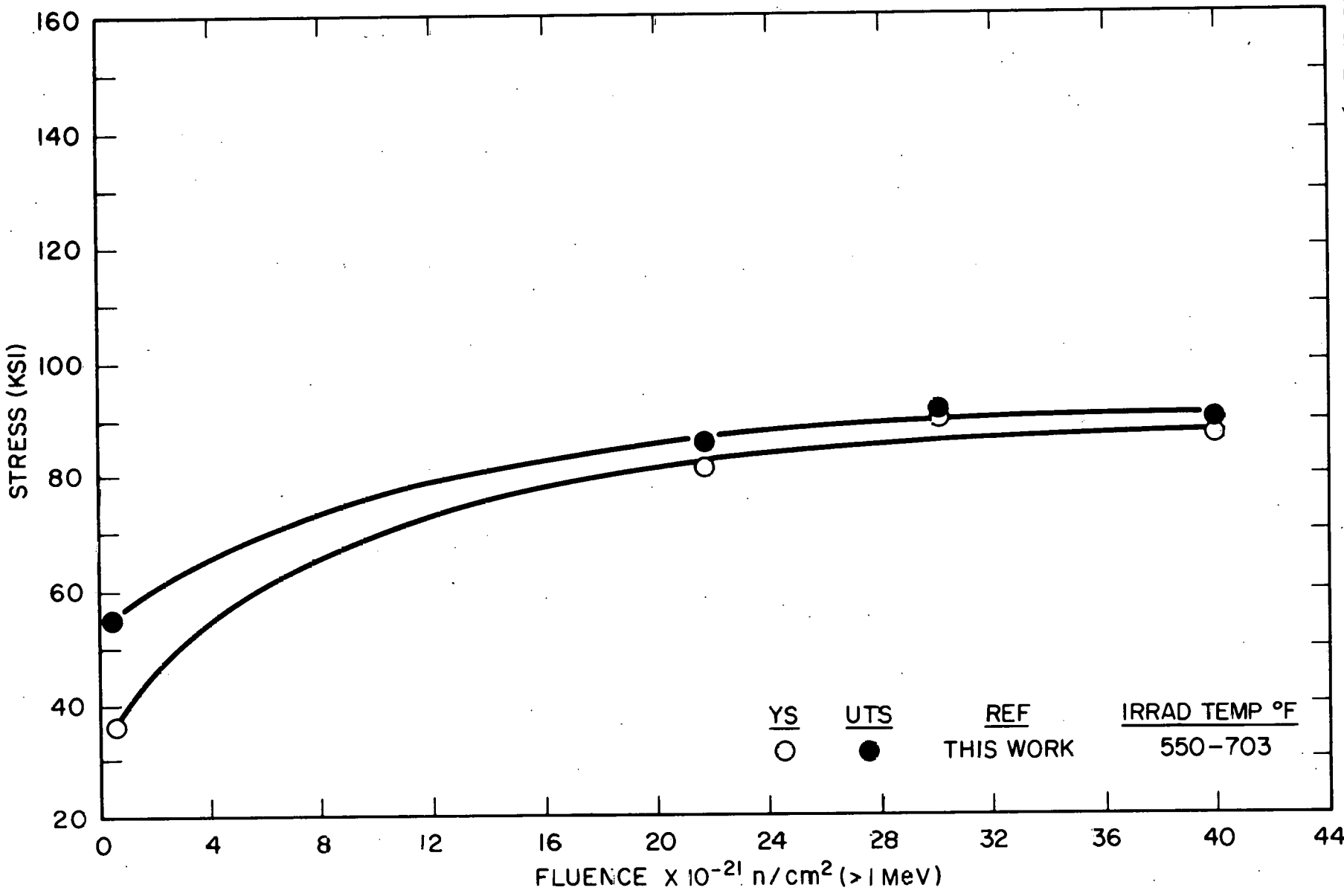

FIGURE 11 - Effect of Fast Fluence on the 1000°F Yield and Ultimate Tensile Strength of Type 347 Stainless Steel

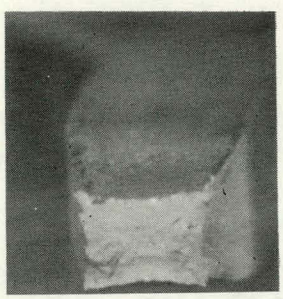

a

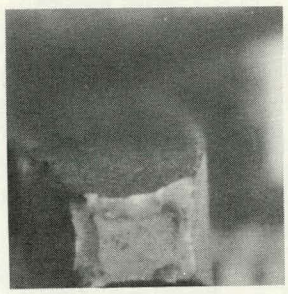

b

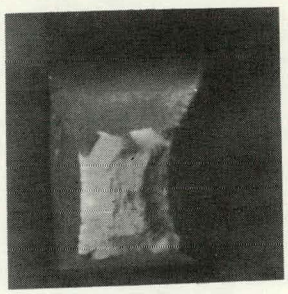

c

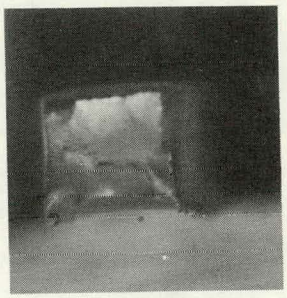

d

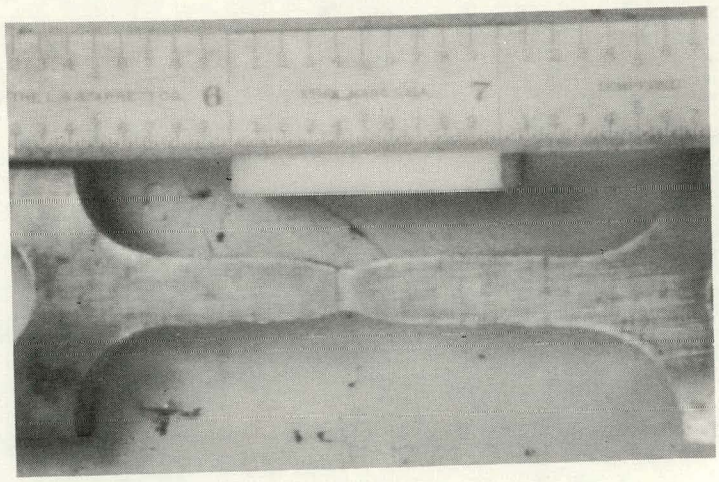

e

Figure 12 - Typical Tensile Fracture Surfaces (4.4X), and Necked Region. (a) Specimen HC2, 3.98 x 10^{22} n/cm^2, (b) HE1, 3.65 x 10^{22} n/cm^2, (c) HH5, 2.22 x 10^{22} n/cm^2, (d) HZ1, .0004 x 10^{22} n/cm^2, (e) HC2, 3.98 x 10^{22} n/cm^2.

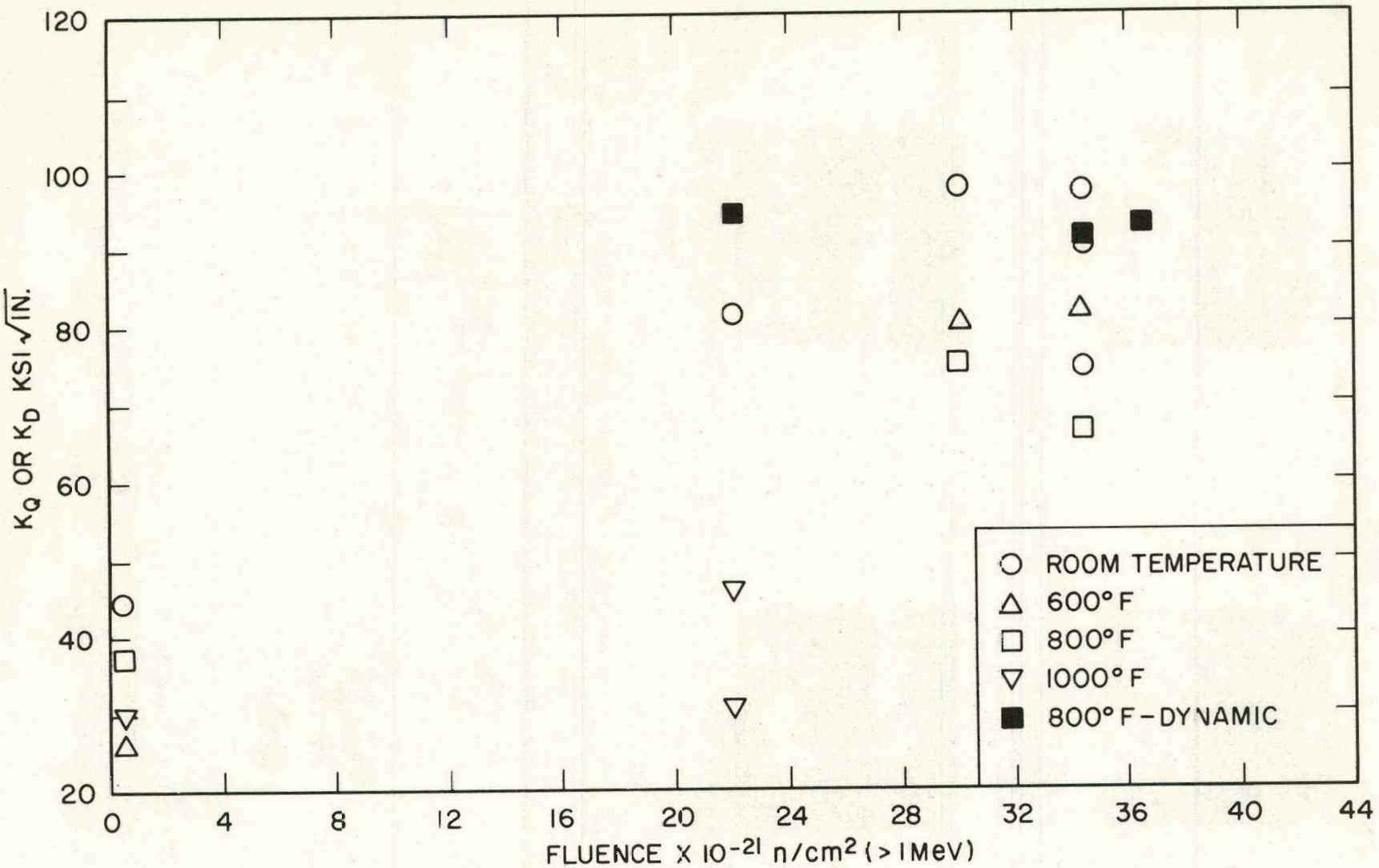

FIGURE 13 - The Effect of Irradiation on the Fracture Toughness Properties of Type 347 Stainless Steel In-Pile Tubes

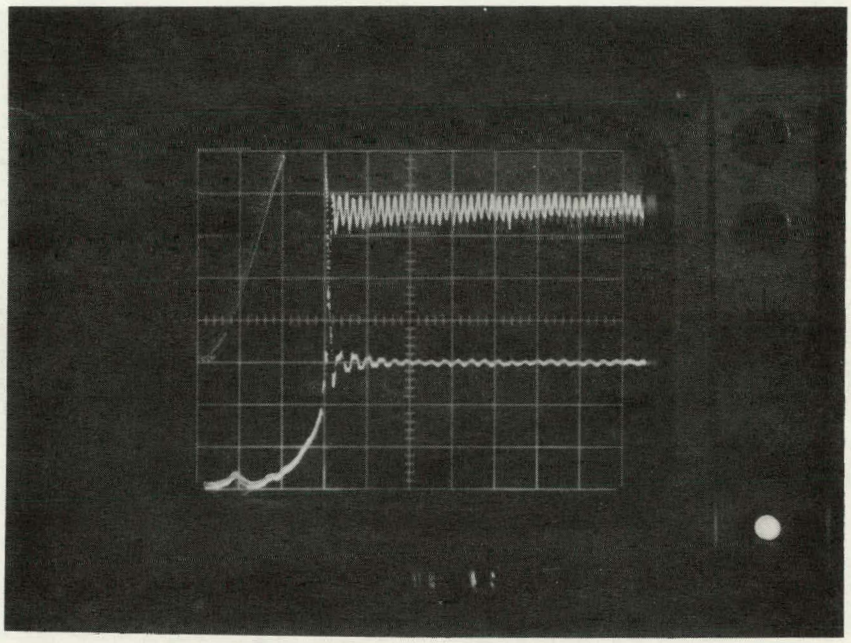

X-AXIS : Time Base : 10 msec/division

Y-AXIS : CH1 (Upper Trace) : Load : 1000 lb/division
CH2 (Lower Trace) : Displacement : 0.020 in/division

Figure 14 Oscilloscope Trace of Dynamic Fracture Toughness Test of Specimen HD5

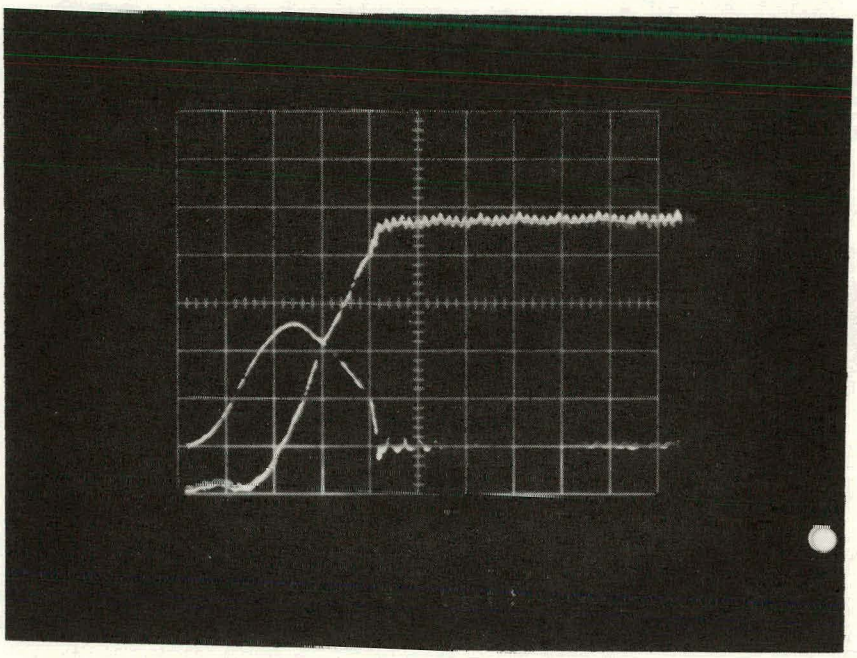

X-AXIS : Time Base : 10 msec/division

Y-AXIS : CH1 (Upper Trace) : Load : 2000 lb/division
CH2 (Lower Trace) : Displacement: 0.020 in/division

Figure 15 Oscilloscope Trace of Dynamic Fracture Toughness Test of Specimen HA4

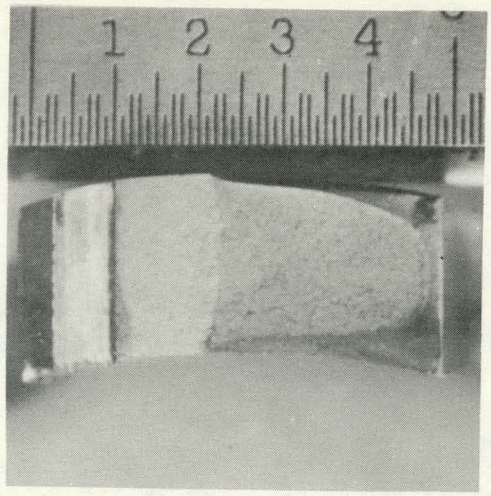

a

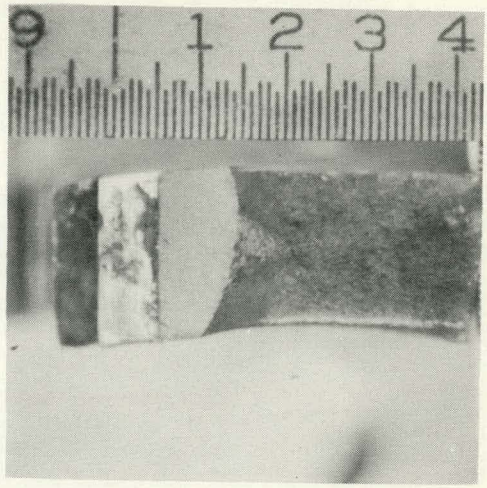

b

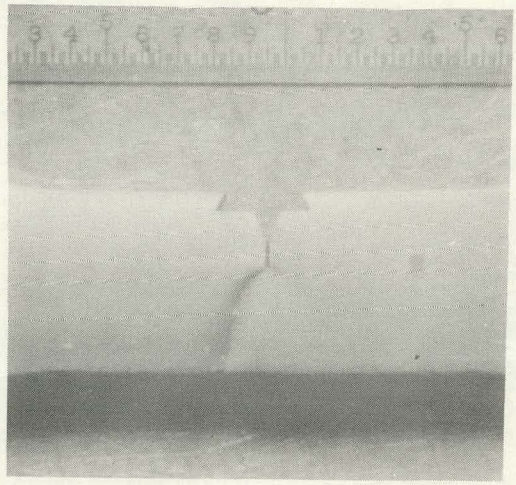

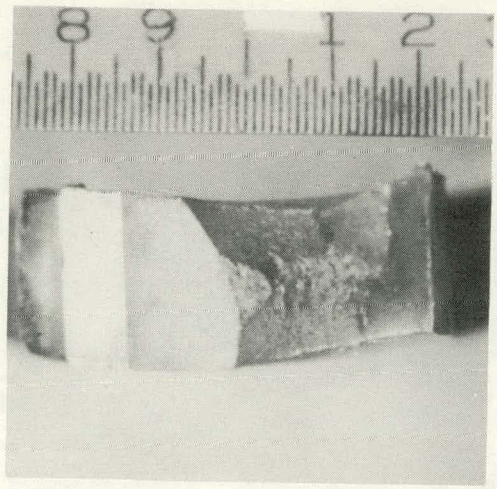

d

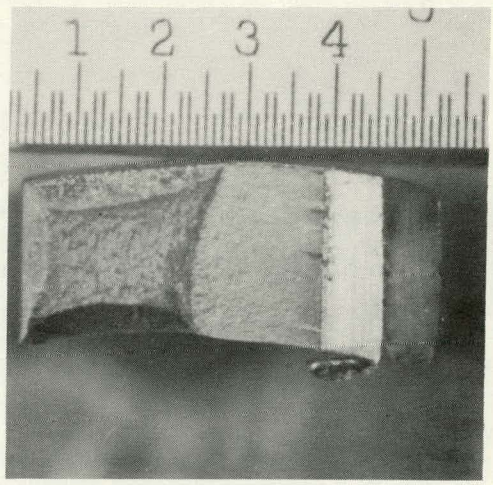

e

Figure 16 - Fracture Toughness Test Fracture Surfaces (4.4X), and Side View of Crack. (a) Specimen HD4, 3.44 x 10^{22} n/cm^2, static test; (b) and (c), HD5, 3.44 x 10^{22} n/cm^2, dynamic test; (d) HA4, 2.20 x 10^{22} n/cm^2, dynamic test; (e) HY2, .0001 x 10^{22} n/cm^2, static test

*U.S. GOVERNMENT PRINTING OFFICE: 1979-603-014/888